Antitumor Imidazotetrazines. 32.[1] Synthesis of Novel Imidazotetrazinones and Related Bicyclic Heterocycles To Probe the Mode of Action of the Antitumor Drug Temozolomide

A. S. Clark,[†] B. Deans,[†] M. F. G. Stevens,*[,‡] M. J. Tisdale,[†] R. T. Wheelhouse,[‡] B. J. Denny,[‡] and J. A. Hartley[§]

Pharmaceutical Sciences Institute, Aston University, Aston Triangle, Birmingham B4 7ET, U.K., Cancer Research Laboratories, Department of Pharmaceutical Sciences, University of Nottingham, Nottingham NG7 2RD, U.K., and Department of Oncology, University College London Medical School, London W1P 8BT, U.K.

Received November 23, 1994[⊗]

A series of new imidazo[5,1-*d*]-1,2,3,5-tetrazinones with additional hydrogen-bonding or ionic substituents at the 8-carboxamide position of the antitumor drugs temozolomide (**1**) and mitozolomide (**2**) has been prepared. None of these compounds were significantly more cytotoxic *in vitro* against the mouse TLX5 lymphoma than the lead structures. Molecular modeling techniques have been used to design benzo- and pyrazolo[4,3-*d*]-1,2,3-triazinones bearing carboxamide groups in appropriate positions which are isosteric with temozolomide and mitozolomide but which cannot ring open to alkylating species. As predicted, these compounds have no inhibitory properties against human GM892A or Raji cell lines *in vitro*. Temozolomide and the spermidine–temozolomide conjugate **28** preferentially methylate guanines within guanine-rich sequences in DNA, but no experimental evidence has been found to support the hypothesis that such regions are involved in catalyzing the ring opening of the imidazotetrazinone prodrugs to their active forms.

Introduction

The chemical mechanism underlying the antitumor properties of temozolomide (**1**) and mitozolomide (**2**) (Figure 1) is reasonably clear. Temozolomide is a prodrug which undergoes base-catalyzed hydrolytic ring opening followed by loss of a molecule of carbon dioxide to generate 5-(3-methyltriazen-1-yl)imidazole-4-carboxamide (MTIC, **4**);[2] this further fragments to the methyldiazonium species **6** as the proximal DNA-methylating agent (Scheme 1).[5] Of the atoms making up the temozolomide ring, N-2 and N-3 are lost as a molecule of nitrogen; C-4 is processed to a molecule of carbon dioxide; and N-1 and all the imidazole ring atoms are eliminated as 5-aminoimidazole-4-carboxamide (**5**, AIC). Thus temozolomide can be considered as a small molecular weight drug-delivery device able to transfer an electrophilic methyl group to vulnerable sites within tumor cells.[5] However, we have not yet found a convincing explanation for the biological inactivity of the 3-ethylimidazotetrazinone **3** (ethazolastone), which has an identical ring-opening chemistry to temozolomide and mitozolomide.[2]

More tentatively, we proposed[5] that runs of guanine residues represent an accessible nucleophilic and basic microenvironment in DNA which would facilitate sequence-selective conversion of the prodrug temozolomide to MTIC, possibly by an 'activated' water molecule in the major groove of DNA. This proposal was supported by molecular modeling studies which indicated that temozolomide could make a productive hydrogen-bonded association with DNA in which the role of the carboxamide group may be crucial in orienting the drug molecule at guanine–cytosine sites.[5] Structure–activity relationships (SAR) in the imidazotetrazine series,[6] as well as the clinical properties of temozolomide itself,[7,8] can be rationalized in terms of this model.

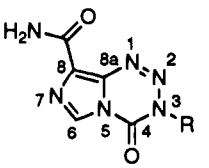

1 R = Me (temozolomide)
2 R = $(CH_2)_2Cl$ (mitozolomide)
3 R = Et (ethazolastone)

Figure 1. Chemical structures of temozolomide, mitozolomide, and ethazolastone.

Scheme 1

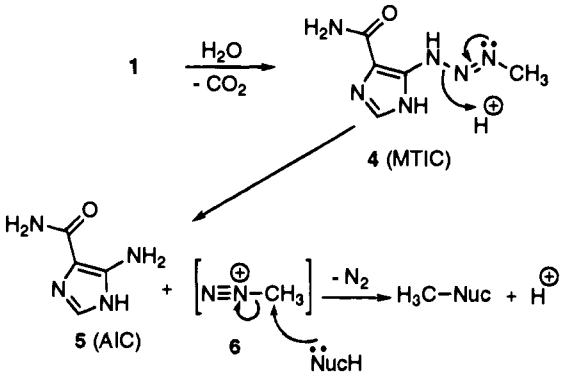

The fact that the unstable species MTIC preferentially methylates the N-7 residue of the middle guanine in runs of guanines in isolated DNA[9] rather confuses the picture. It is clear, however, that the antitumor properties of temozolomide correlate with methylation at O-6 guanine sites, since tumor lines expressing high levels of the O^6-alkyl-DNA alkyltransferase repair protein are refractory to treatment by temozolomide.[10,11]

* Address for correspondence: Cancer Research Laboratories, Department of Pharmaceutical Sciences, University of Nottingham.
[†] Aston University.
[‡] University of Nottingham.
[§] University College London Medical School.
[⊗] Abstract published in *Advance ACS Abstracts*, March 15, 1995.

0022-2623/95/1838-1493$09.00/0

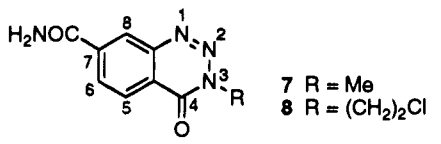

7-Carbamoylbenzo-1,2,3-triazinones

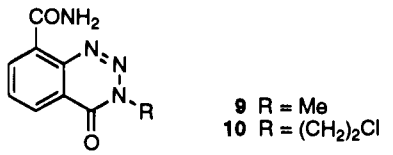

8-Carbamoylbenzo-1,2,3-triazinones

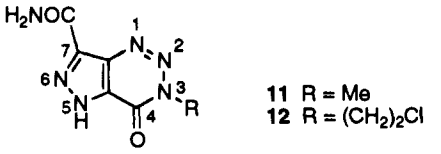

7-Carbamoylpyrazolo[4,3-*d*]-1,2,3-triazinones

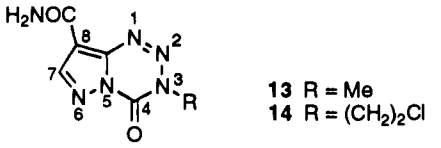

8-Carbamoylpyrazolo[5,1-*d*]-1,2,3,5-tetrazinones

Figure 2. Structural analogues of antitumor imidazotetrazinones.

In this paper we give details of molecular modeling, synthesis, cytotoxicity, and sequence-selective DNA binding of compounds of two types designed to examine the validity of the overall working hypothesis. These are imidazotetrazinones bearing hydrogen-bonding and polyamine functionalities attached to the 8-carboxamide residue which could extend the DNA sequence tract recognized by this class of agent and bicyclic heterocycles bearing carboxamide groups which, although sterically and electronically related to temozolomide and mitozolomide, are unable to ring open to alkylating species. We envisaged that these molecular probes (see Figure 2 for structures) might compete for imidazotetrazine recognition sites on DNA, if such *loci* exist, and that this competition might antagonize the activity of temozolomide in a susceptible cell line.

Results and Discussion

Molecular Modeling. Data for the electrostatic similarities and calculated atomic charges at C-4 of the tetrazinone or triazinone rings are shown in Table 1. Based solely on shape, all compounds might be expected to mimic closely temozolomide and mitozolomide; whereas in terms of electrostatic potentials, only the pyrazolotriazinones **11** and **12** (HPSI of 0.933 and 0.919, respectively) were predicted to be similar to the lead structures. However, since active imidazotetrazinones only expose their cytotoxicity after ring opening at C-4,[2-5] calculation of the electron density at this site was a crucial factor in predicting activity. In this respect the pyrazolotetrazinones **13** and **14** have a theroretical partial charge at C-4 equivalent to the active imidazotetrazinones, and indeed compound **14** displays anti-tumor activity in mouse tumor models *in vivo* on par with mitozolomide (**2**).[14]

Table 1. Similarities of Shape, Electrostatic Potentials, and Atomic Charges at C-4 for Imidazo- and Pyrazolo[5,1-*d*]-1,2,3,5-tetrazinones and Benzo- and Pyrazolo-1,2,3-triazinones

compd	shape[a]	HPSI[a]	atomic charge at C-4
1			0.417
2			0.416
7	0.963	0.644	0.325
8	0.965	0.646	0.325
9	0.966	0.789	0.327
10	0.970	0.791	0.325
11	0.999	0.933	0.319
12	0.997	0.919	0.313
13	0.997	0.857	0.409
14	0.995	0.831	0.411

[a] Compounds **7**, **9**, 11, and **13** are compared with temozolomide (value 1) and compounds **8**, **10**, **12**, and **14** with mitozolomide (value 1).

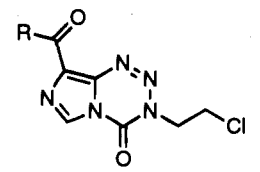

20 R = OH
21 Cl
22 NHPh
23 $NHC_6H_4.CONH_2$-*o*
24 $NHC_6H_4.CONH_2$-*m*
25 $NHC_6H_4.CONH_2$-*p*
26 $NHC_6H_3.(CONH_2)_2$-*o and p*

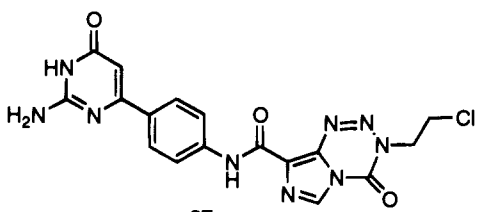

27

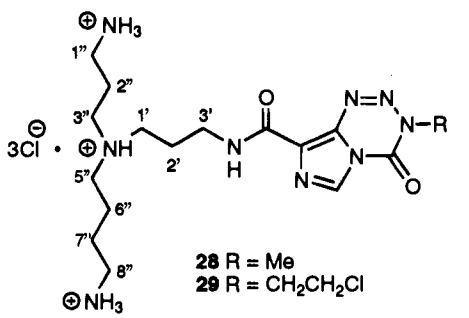

28 R = Me
29 R = CH_2CH_2Cl

Figure 3. Structures of imidazotetrazinones conjugated to substituted anilines and spermidine in the 8-position.

Chemistry. We have synthesized a series of substituted 8-carboxanilides, **23**–**26**, bearing an additional carboxamide group (Figure 3) to explore the biological outcome of increasing hydrogen-bonding potential at the 8-position. We have also synthesized imidazotetrazinones conjugated to spermidine through an 8-(3-aminopropyl)carboxamide linkage. The second objective of the present work was to synthesize *nonalkylating* analogues which might compete with active imidazotetrazinones for putative DNA binding sites: our efforts have focused on bicyclic heterocycles lacking the bridgehead nitrogen atom, ie., the benzo-1,2,3-triazinones **9** and **10** and pyrazolo[4,3-*d*]-1,2,3-triazinones **11** and **12**.

Scheme 2

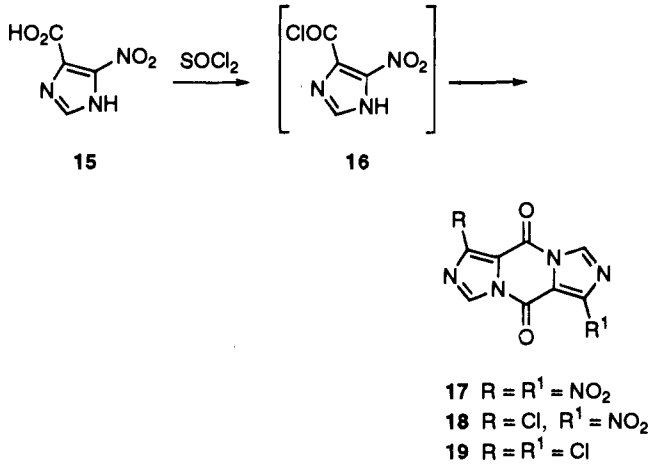

15 16

17 R = R¹ = NO₂
18 R = Cl, R¹ = NO₂
19 R = R¹ = Cl

In an earlier paper[14] we showed that 5-nitroimidazole-4-carboxylic acid (**15**) did not form the isolatable acid chloride **16** when treated with thionyl chloride or phosphorus pentachloride: instead, the previously reported tricyclic lactam **17** was formed (Scheme 2).[15] This lactam ring opened in the presence of primary and secondary amines to give poor yields of substituted 5-nitroimidazole-4-carboxamides which were subsequently transformed to imidazotetrazines.[14,16] In the present work we intended to exploit reactions of **17** with more complex amines but found that newly synthesized samples were contaminated with significant amounts of the chloro nitro lactam **18** and the dichloro lactam **19**. The crude products showed a molecular ion for compound **17** at 278 *m/z* and major peaks at 267/269 and 256/258/260 *m/z* for the monochloro (**18**) and dichloro (**19**) lactams, respectively. These impurities presumably account for the low yields recorded previously. Efforts to improve the yield of the dinitro lactam **17** by conducting the thionyl chloride/phosphorus pentachloride cyclizations under milder conditions, or by separating it from the mixture, were not successful.

As an alternative approach, mitozolomide (**2**) was converted to the carboxylic acid **20** and then to the acid chloride **21**.[16] Reaction of the acid chloride with aniline and a series of carbamoyl-subsituted anilines afforded the anilides **22**–**26** in poor yields. The pyrimidinylanilinoimidazotetrazine **27** was synthesized in 28% yield from the acid chloride **21** and 2-amino-6-(4-aminophenyl)pyrimidin-4-one and crystallized as a solvate with 1-methylpyrrolidin-2-one. The spermidine conjugates **28** and **29** of temozolomide and mitozolomide were prepared by reacting the appropriate imidazotetrazine acid chlorides with N^1,N^8-bis(*tert*-butoxycarbonyl)-N^4-(3-aminopropyl)spermidine followed by deprotection and isolation of the trihydrochloride salts: the hygroscopic nature of the salts dictated characterization by high-field NMR and accurate-mass FAB mass spectrometry.

Syntheses of 7- or 8-carbamoyl-1,2,3-benzotriazin-4(3*H*)-ones **36** and **37** were accomplished in three high-yielding steps starting from the nitrobenzenedicarboxylic acids **31** and **30** (Scheme 3). These were converted to the amides **32** and **33** with thionyl chloride and ammonia, catalytically reduced to the amines **34** and **35**, and cyclized to the benzotriazinones **36** and **37**.

Selective alkylation at the 3-position of the benzotriazinone substrates **36** and **37** did not seem a practical

Scheme 3

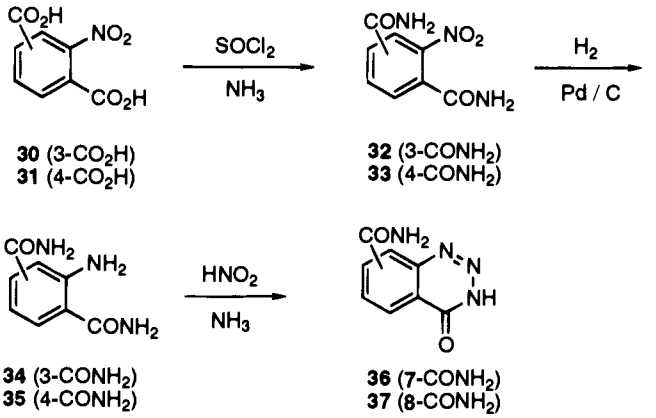

30 (3-CO₂H)
31 (4-CO₂H)

32 (3-CONH₂)
33 (4-CONH₂)

34 (3-CONH₂)
35 (4-CONH₂)

36 (7-CONH₂)
37 (8-CONH₂)

proposition on the basis of earlier experiences,[17] and a modified strategy was necessary to incorporate a range of substituents at this site (Scheme 4). Thus, the dicarboxylic acids **30** and **31** were firstly hydrogenated to give the amines **38** and **39** and converted to the isatoic anhydrides **40** and **41** with triphosgene. Selective ring opening at C-4 yielded the substituted amides **42**–**49** which were cyclized to the benzotriazinonecarboxylic acids **50-57** by nitrosation. The carboxylic acids were converted with thionyl chloride and ammonia to two series of benzotriazinones, bearing carboxamide groups at the C-7 (**7, 58, 59**) or C-8 positions (**9, 10, 60**–**62**). During the ammonolysis step, the methyl ester group of compound **56** was converted to an amide in **61**.

An alternative route to the 7-carbamoyl-3-methylbenzo-1,2,3-triazinone **7** started with the substituted methyl anthranilate **63** which was diazotized and coupled with methylamine or aniline to afford the triazenes **64** and **65** in 70% and 80% yields, respectively (Scheme 5). The ^{1}H NMR spectrum of the methyltriazene **64** in $CDCl_3$ showed the *N*-methyl resonance as a singlet at δ 3.60, suggesting that it exists as the methylazo tautomeric form,[18] probably preferred because of stabilization by intramolecular hydrogen bonding.[19] Cyclization of the triazenes in boiling 95% ethanol afforded the benzotriazinones **66** and **67** in 75% yields, and ammonolysis of the ester **66** yielded the carboxamide **7**, identical to the sample prepared by the isatoic anhydride route. Incorporation of 2% piperidine in the cyclization of the phenyltriazene **65** in ethanol led to ester exchange and isolation of the ethyl ester **68** in 66% yield. Similarly, treatment of triazene **65** with 70% aqueous methanol containing 2% piperidine led to the isolation of the benzotriazinonecarboxylic acid **52**.

We were unable to synthesize the carbamoylpyrazolotriazinone **11**. In the closest attempt, the pyrazole dimethyl ester **69** was converted to the diazopyrazole **70** and immediately reacted with excess anhydrous methylamine in ethyl acetate solution; the product was the methylcarboxamide **72** (5%), probably formed *via* an intermediate (methyltriazenyl)pyrazole, **71** (Scheme 6). Finally, the 3-benzylpyrazolotetrazinone **74** was synthesized in 85% yield by reacting the diazopyrazole **73** with benzyl isocyanate.

Hydrolysis of Mitozolomide. The rate of hydrolysis of imidazotetrazines is strongly influenced by pH.[2,5] Initial experiments were conducted in which hydrolytic degradation of mitozolomide **2** was examined in different solutions at pH 7.4 at 37 °C which contained the

Scheme 4

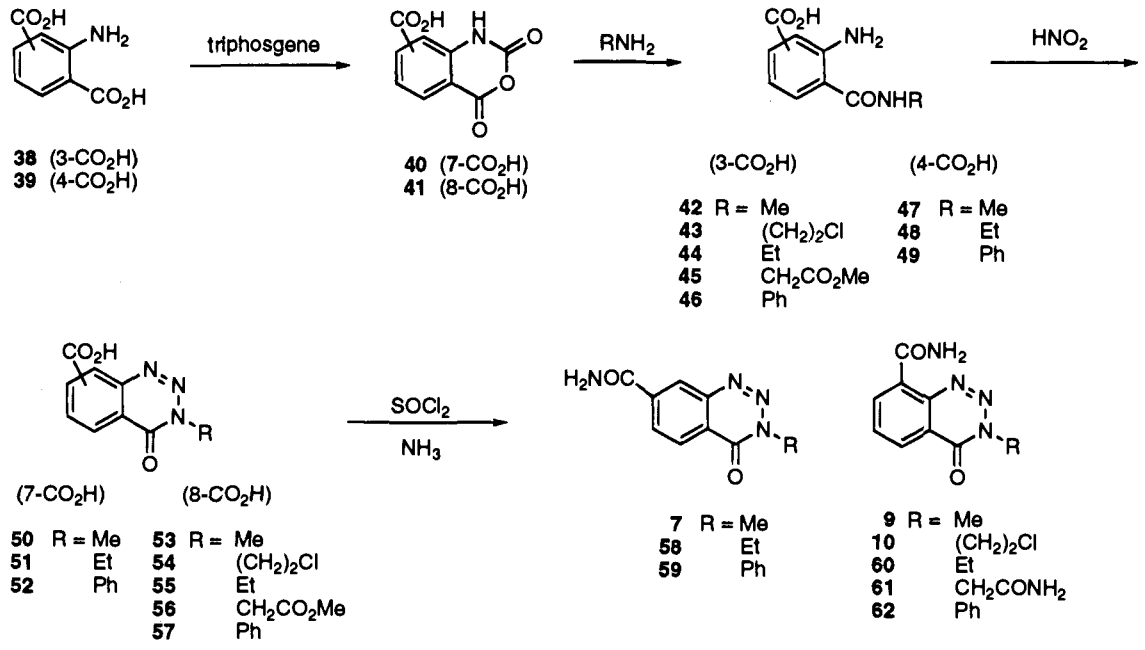

Scheme 5

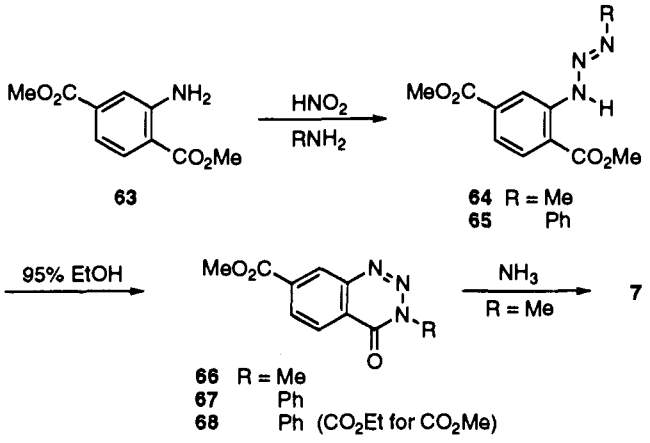

Scheme 6

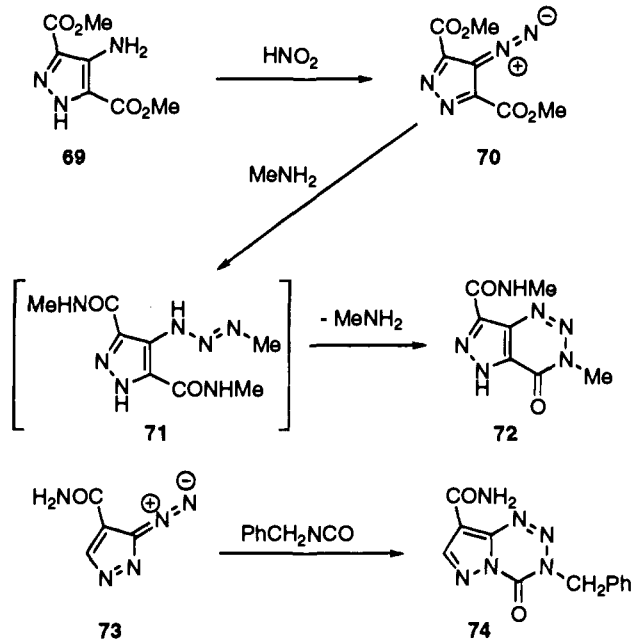

following: (a) phosphate buffer (0.1 M) which acted as a positive control in the measurement of the rate of pH dependent hydrolysis (k_{pH}), (b) a solution of d(G)-d(C) homopolymer in phosphate buffer, (c) an equimolar solution of guanosine-5′-monophosphate and cytidine-5′-monophosphate in phosphate buffer to measure any catalytic influence of individual components of G-C DNA, and (d) a solution of d(A)-d(T) homopolymer in phosphate buffer which acted as a control to monitor whether any observed catalytic effect was confined to G-C-rich DNA or DNA as a whole.

Mitozolomide was incubated with two concentrations of the oligonucleotide solutions, an equimolar concentration and a 10 mole excess of oligonucleotide. Disappearance of mitozolomide was monitored by HPLC,[20] and hydrolysis was found to follow pseudo-first-order kinetics: the rate constants (k) were obtained from plots of log(mitozolomide peak area) versus time that were linear to three half-lives (data not shown). Values for k and calculated half-lives ($t_{1/2}$) are shown in Table 2. There was no significant difference between the $t_{1/2}$ values in phosphate buffer (A) at pH 7.4 alone or in buffer containing G-C or A-T oligonucleotides or component G and C nucleotides.

In order to examine the possibility that the pH dependent hydrolysis in the presence of the phosphate nucleophile might dominate any effects associated with the presence of the oligonucleotide (i.e., $k_{pH} > k_{G\text{-}C}$), decompositions were also conducted in phosphate buffer at pH 6.5 and sodium cacodylate buffer at pH 7.4 and 6.5. Again there was no difference in the $t_{1/2}$ values in buffered solution alone and in the presence of oligonucleotides (Table 3). However there was a moderate increase in the rate constants for the degradation of mitozolomide in cacodylate buffer compared with those in phosphate buffer suggesting that the large mole excesses of nucleophiles in the buffers may be masking any effects due to the interactions of the drug with oligonucleotides in these experiments.

***In Vitro* Cytotoxicity of Imidazotetrazinones and Related Compounds.** The cytotoxicities of several compounds prepared in this work were tested *in*

Table 2. First-Order Rate Constants (k) and Half-Lives ($t_{1/2}$) for the Hydrolysis of Mitozolomide (**2**) in Buffers at Different pH Values at 37 °C in the Presence of Oligonucleolides and Nucleotides

incubation mixture	buffer	pH	rate constant ($k \times 10^3$ min^{-1})[a] 1	2	3	mean rate constant ($\times 10^3$ min^{-1})	half-life, $t_{1/2}$ (min)[b]
control[c]	A	7.4	9.74	9.51	9.82	9.69 ± 0.18	71.5
d(G)-d(C) (1:1)[d]	A	7.4	9.39	9.30	9.68	9.40 ± 0.28	73.3
d(G)-d(C) (10:1)[e]	A	7.4	8.68	9.29	9.35	9.11 ± 0.43	76.1
5′-GMP/5′-CMP (1:1)[f]	A	7.4	9.79	9.86	9.72	9.79 ± 0.07	70.8
d(A)-d(T) (1:1)[d]	A	7.4	8.95	9.34	9.15	9.15 ± 0.20	75.8
d(A)-d(T) (10:1)[e]	A	7.4	9.23	9.30	9.38	9.32 ± 0.09	74.4
control[c]	B	6.5	1.52	1.53	1.51	1.52 ± 0.01	456.0
d(G)-d(C) (10.1)[e]	A	6.5	1.54	1.54	1.53	1.54 ± 0.01	450.0
d(A)-d(T) (10.1)[e]	B	6.5	1.54	1.55	1.55	1.55 ± 0.01	447.2
control[c]	C	7.4	12.5	12.2		12.4 ± 0.2	55.9
d(G)-d(C) (10:1)[e]	C	7.4	11.7	12.7		12.2 ± 0.5	56.8
d(A)-d(T) (10:1)[e]	C	7.4	11.0	13.4		12.2 ± 1.2	56.8
control[c]	D	6.5	2.01	2.05		2.03 ± 0.02	341.5
d(G)-d(C) (10:1)[e]	D	6.5	2.01	2.00		2.01 ± 0.01	344.8
d(A)-d(T) (10:1)[e]	D	6.5	2.02	1.97		2.00 ± 0.03	346.6

[a] Calculated from plots of log(mitozolomide peak area) versus time with a minimum of 10 data points. [b] Calculated from the mean rate constant using the equation $t_{1/2} = 0.693/k$. [c] Buffer solution only. Buffers: A, phosphate buffer (0.1 M) at pH 7.4; B, phosphate buffer (0.1 M) at pH 6.5; C, sodium cacodylate buffer (0.1 M) at pH 7.4; D, sodium cacodylate buffer (0.1 M) at pH 6.5. [d] Equimolar ratio of mitozolomide to nucleotide bases in the oligonucleotide. [e] Ten-fold mole excess of nucleotide bases in the oligonucleotide compared to mitozolomide. [f] Represents equimolar ratios of guanosine-5′-monophosphate to cytidine-5′-monophosphate.

Table 3. *In Vitro* Cytotoxicity of Imidazo[5,1-*d*]-1,2,3,5-tetrazinones and Benzo-1,2,3-triazinones against Mouse TLX5 Lymphoma Cells

compd	IC_{50} (μM)[a]
1 (temozolomide)	5.0
2 (mitozolomide)	2.5
7	380
8	350
9	>500
10	225
20	15.8
22	1.25
23	13
24	35
25	37
26	375
27	25
37	400
58	108
59	140
60	325
61	>500
62	>500

[a] Results are the mean of two separate determinations.

vitro against the mouse TLX5 lymphoma, a cell line which has proved valuable in evaluating SAR in imidazotetrazines.[2,14,16] The reference compounds were temozolomide (**1**) and mitozolomide (**2**) which gave IC_{50} values of 5 and 2.5 μM, respectively. As predicted from the modeling studies, representative 1,2,3-benzotriazinones **7**–**10**, **37**, and **58**–**62** were generally at least 100-fold less cytotoxic than mitozolomide and had IC_{50} values in the range 100–>500 μM (Table 3). The carboxanilide **22** was equipotent with mitozolomide but attachment of an additional carboxamide residue to the anilide fragment **23**–**25** reduced activity approximately 10-fold; incorporation of two carboxamide groups furnished a compound, **26**, which was extremely insoluble and inactive. Activity was only partially restored in the substituted aminopyrimidinone-conjugated mitozolomide **27** (IC_{50} = 25 μM) despite the potential of this compound to undergo Watson–Crick type hydrogen bonding to guanine and cytosine residues in single-stranded DNA or Hoogsteen bonding to duplex DNA.[21]

Drug cytotoxicity has also been determined in two cell lines differing in their capacity to effect repair of O^6-alkylguanine lesions, the O^6-alkylguanine-DNA alkyltransferase deficient (Mer$^-$) human lymphoblastoid cell line GM892A and the repair proficient (Mer$^+$) Raji cell line originally obtained from a patient with Burkitt's lymphoma.[22] IC_{50} values determined from growth inhibition assays are recorded in Table 4. For the reference imidazotetrazinones, the order of potency was mitozolomide > temozolomide > ethazolastone. The Mer$^-$ cell line was 23- and 8-fold more sensitive to temozolomide and mitozolomide, respectively, than the Mer$^+$ Raji line, whereas ethazolastone showed only a 2-fold differential between the two cell lines. MTIC (**4**), the intermediate generated upon ring opening of temozolomide, also showed high potency and discriminating activity, as did the mutagenic agent *N*-methyl-*N*′-nitro-*N*-nitrosoguanidine (MNNG); the related methylating agent *N*-methyl-*N*-nitrosourea (MNU) was less potent but still showed a 7.5-fold greater activity against the Mer$^-$ cell line. These data can be explained by the fact that all three agents are themselves progenitors of a common methyl transfer agent, the methyldiazonium cation **6**, which can alkylate a variety of sites on DNA including O-6 and N-7 of guanine.[5] Puzzlingly, the antimelanoma drug 5-(3,3-dimethyltriazen-1-yl)imidazole-4-carboxamide (DTIC) also displayed moderate potency against the GM892A cells and 9-fold selectivity

Table 4. *In Vitro* Cytotoxicity of Imidazo- and Pyrazolo[5,1-*d*]-1,2,3,5-tetrazinones, Benzo- and Pyrazolo-1,2,3-triazinones, and Reference Compounds against GM892A (Mer$^-$) and Raji (Mer$^+$) Cells

compd	IC_{50} (μM)[a] GM892A	Raji	ratio of IC_{50}, Raji/GM892A
1 (temozolomide)	7.6 ± 1.5	175 ± 7	23.0
2 (mitozolomide)	4.8 ± 0.4	39 ± 6	8.1
3 (ethazolastone)	180 ± 12	435 ± 33	2.4
4 (MTIC)	5 ± 2	101 ± 16	20.6
MNNG	0.2 ± 0.07	2.0 ± 0.4	10.0
MNU	35 ± 9	259 ± 28	7.4
DTIC	14 ± 6	128 ± 10	9.0
7	>500	>500	
9	>500	>500	
13	5.3 ± 0.8	270 ± 15	51
28	>500	>500	
72	>500	>500	

[a] Mean ± SEM for at least three determinations.

in favor of the Mer⁻ cells despite the accepted view that this agent requires prior metabolic demethylation to exert a cytotoxic action.[23] Possibly the GM892A cells can effect this transformation even *in vitro*.

In our hands the 3-methylpyrazolotetrazinone **13** showed impressive *in vitro* potency and selectivity, with a 50-fold differential toxicity toward the Mer⁻ cell line. The latter result contrasts with the reported inactivity of this methylpyrazolo-tetrazinone against mouse tumors *in vivo*[24] whereas the 3-(2-chloroethyl) analogue **14** is very active.[14] The spermidine–temozolomide conjugate **28** had low cytotoxicity against both GM892A and Raji cells (IC_{50} > 500 μM).

As expected, none of the new 1,2,3-triazinones (**7**, **9**, and **72**) showed useful activity against either cell line with IC_{50} values > 500 μM (Table 4). Competition assays were performed to assess the ability of these stable compounds to antagonize the cytotoxic action of temozolomide. Preincubation of GM892A cells for 2 h with the 7- or 8-carbamoylbenzo-1,2,3-triazinone **7** or **9** did not inhibit the cytotoxic properties of temozolomide (data not shown) suggesting that these compounds do not compete with the drug for uptake into cells or for binding sites in DNA.

DNA Footprinting Studies. Various DNA footprinting techniques were employed in attempts to determine potential binding sites for temozolomide, but these studies were not successful. Briefly, a homogeneous sample of a labeled 150-base pair *Tyr* T DNA fragment[25] was digested by DNAase I in the presence and absence of drugs, and the fragments were visualized by autoradiography following electrophoresis. Whereas the model drug echinomycin, at 100 μM, showed DNA binding sites as distinct gaps near positions 35, 55, 75, and 100 corresponding to sections where the DNA remained uncut by DNAase I, there were no observable differences from solvent controls for DNA digested in the presence of temozolomide (**1**) or MTIC (**4**) at 4 or 37 °C with drug concentrations in the range 20 μM to 1 mM (data not shown). Similarly, the benzotriazinones **7** and **9** showed no impedance to DNAase I-mediated DNA cleavage.

Further footprinting studies were performed using a modification of the Maxam and Gilbert sequencing technique to examine the ability of drugs to protect DNA from alkylation.[26] Temozolomide did not protect guanine residues from dimethyl sulfate methylation, nor did temozolomide or MTIC preserve guanine residues from diethyl pyrocarbonate ethylation (data not shown). Thus, if an imidazotetrazinone specific receptor site did exist, these footprinting techniques appeared unable to aid clarification of such interactions.

Sequence Specificity of Covalent Modification of DNA. In order to examine the DNA sequence selectivities of temozolomide (**1**), the pyrazolotetrazinone isostere **13** and the spermidine–temozolomide conjugate **28**, a modification of the standard Maxam and Gilbert sequencing technique was used to examine guanine N-7 alkylation. 5′-End-labeled *Bam*HI-*Sal*I DNA fragments were incubated with drug at 37 °C for 2 h, and the DNA was cleaved with piperidine to produce breaks at sites of guanine N-7 alkylation. The patterns of fragments obtained are shown (Figure 4). Results are compared with those from two related compounds devoid of antitumor activity—ethazolastone (**3**) and the 3-benzylpyrazolotetrazinone **74**.

Bands predominated at sites corresponding to runs of three or more contiguous guanine bases indicating temozolomide, the pyrazole analogue **13**, and the spermidine conjugate **28** do preferentially alkylate these sites. Ethazolastone (**3**) and the benzylpyrazolotetrazinone **74** were less discerning. In addition, qualitative examination of the level of fragment cleavage following alkylation indicates ethazolastone to have very low reactivity (Figure 4A, lanes a, b) by comparison with temozolomide (lanes c–g), a factor which may contribute to the lack of antitumor activity of the ethyl congener. It was anticipated that conjugation with spermidine would provide temozolomide with enhanced DNA-directed activity, and a significant increase in DNA reactivity was indeed detected (Figure 4A, lanes h–m). However, initial studies indicated that *in vitro* antitumor activity may not parallel DNA reactivity since at 500 μM the percent control population growth in GM892A and Raji cells was 52.5% and 85%, respectively. Cytotoxicity was not improved by depletion of cellular polyamine levels, using difluoromethylornithine (0.5 mM, 72 h) prior to exposure of these cell lines to the conjugate. Hence, cellular delivery of **28** would appear to be hampered by the necessity for a spermidine uptake mechanism, although this in turn may allow the targeting of tumor cells possessing such an uptake system.[27] Quantitative comparison between the 3-methylpyrazolotetrazinone **13** (Figure 4B, lane c), the 3-benzylpyrazolotetrazinone **74** (lane d), and temozolomide (lane e) shows that even a 10-fold higher concentration of the benzyl compound **74** did not elicit equivalent levels of alkylation as the two methyl compounds.

The piperidine cleavage assay is confined to the detection of guanine N-7 alkylations, and so sequence selectivity was also examined using a primer extension procedure utilizing multiple cycles of polymerization with the thermostable DNA polymerase from *Thermus aquaticus*. Following annealing of a 5′-end-labeled primer to template DNA, extension with *Taq* DNA polymerase produced a full length fragment of 263 bp in a solvent control. The ability of temozolomide alkylations to block the progress of the polymerase, causing premature termination of chain elongation, is presented in Figure 5. Unmodified DNA showed very few sites of early termination, whereas with temozolomide-alkylated DNA termination occurred at guanine bases preferentially in the nucleophilic microenvironment of clustered, rather than isolated, guanines. This confirmed the results of the piperidine cleavage assay and indicated that the major lesion produced by this agent is at the guanine N-7 position.

Conclusions

Earlier structural and bioactivity studies on antitumor imidazotetrazinones conducted with the responsive mouse TLX5 lymphoma demonstated the importance of the hydrogen-bonding property of the 8-carboxamide substituent.[2,4,14,16] However, 8-carboxanilides **23-27** designed to potentially augment bonding at this site were less active than the prototype agents temozolomide (**1**) and mitozolomide (**2**) against this tumor *in vitro*.

Molecular modeling approaches were employed to design bicyclic isosteres of temozolomide and mitozolo-

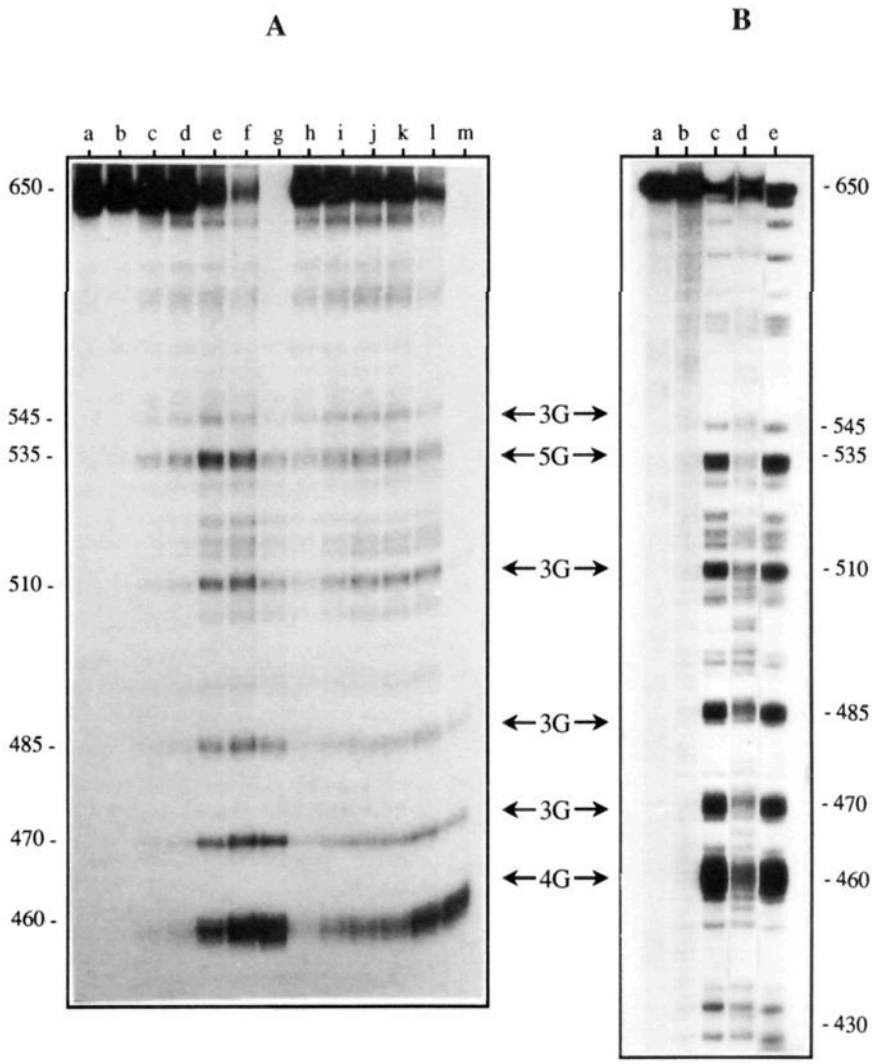

Figure 4. Sites of guanine N-7 alkylation produced in the 276-bp *Bam*HI-*Sal*I fragment of pBR322, 5′-labeled at the *Bam*HI site. (A) Lane (a) 2.5 and (b) 5 mM ethazolastone (**3**); (c) 50 μM, (d) 100 μM, (e) 250 μM, (f) 500 μM, and (g) 1 mM temozolomide (**1**); (h) 2 μM, (i) 10 μM, (j) 50 μM, (k) 100 μM, (l) 500 μM, and (m) 1 mM temozolomide−spermidine conjugate **28**. (B) Lane (a) solvent control; (b) formic acid purine marker lane; (c) 250 μM 3-methylpyrazolotetrazinone **13**; (d) 2.5 mM 3-benzylpyrazolotetrazinone **74**; (e) 250 μM temozolomide. Numbers refer to the base sequence (see the supplementary material) for which sites of three or more contiguous guanine residues are marked.

mide based on benzo- and pyrazolo-1,2,3-triazinones, which cannot ring open to alkylating species; these compounds were not active (IC_{50} > 500 μM) against human GM892A (Mer^-) and Raji (Mer^+) cell lines *in vitro*, nor did they protect these cell lines from subsequent challenge by temozolomide. The lack of potency of the spermidine conjugates **28** and **29** can be attributed to the lack of a polyamine uptake system in these cells.

The rate of ring opening of mitozolomide was significantly influenced by pH ($t_{1/2}$ = 1.25 h at pH 7.4 and 7.5 h at pH 6.5 in phosphate buffer) and the nature of the buffer (phosphate or cacodylate); furthermore, no rate enhancements were observed in the presence of d(G)-d(C) oligonucleotides. This could be due to weak association of the drug with DNA, the consequence being that the reaction in bulk solution dominated any effects due to association with DNA. Further evidence for this weak association came from the failure of footprinting techniques to detect noncovalent associations between temozolomide and DNA. Recent NMR studies (unpublished) further support this hypothesis.

Temozolomide and the spermidine conjugate both preferentially methylated guanine-rich sequences in a *Bam*HI-*Sal*I DNA fragment as determined by piperidine cleavage experiments and induced blocks to *Taq* DNA polymerase action at similar sites. The same sites were also methylated by MTIC (data not shown). Investigations with mitozolomide, its corresponding (chloroethyl)-triazene, and a series of other triazenes[9] have indicated that the imidazocarboxamide group has some influence in determining the fine details of reactivity with DNA although selectivity is mainly a property of the DNA sequence and not the drug. Presentation of the alkylating agent either as imidazotetrazine prodrug or open-chain triazene has no discernable affect on the products of the reaction. Furthermore, the SAR[6] and modeling studies[5] make no proposals for the interaction of temozolomide with DNA which could not also apply to MTIC.

The evidence presented here suggests that the conversion from imidazotetrazinone prodrug to drug occurs in free solution under the influence of local pH[36] rather than in the major groove catalyzed by a target DNA sequence as previously proposed. This theory is in

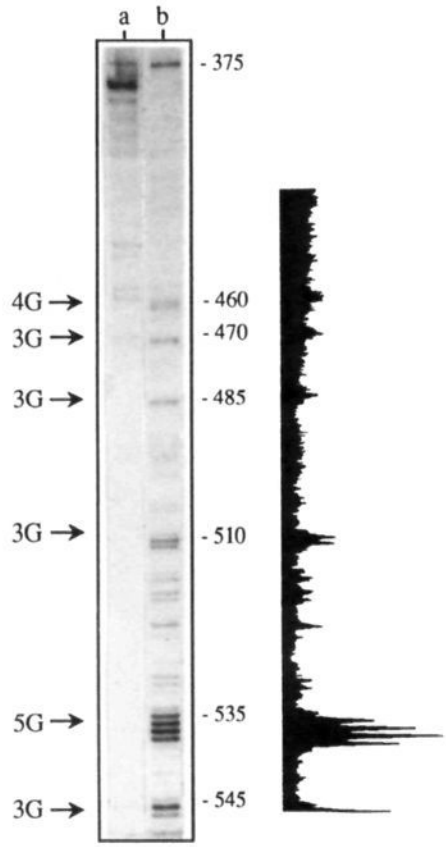

Figure 5. Sequence specificity of covalent adduct formation measured by a *Taq* DNA polymerase stop assay. Bands indicate the sites of termination for extension of a 5′-end-labeled primer complementary to bases 621–640 of the *Bam*HI-*Sal*I fragment of pBR322 (bases 375–650): (a) control unmodified fragment and (b) 1 mM temozolomide (**1**). An optical densitometric scan of lane b is shown on the right. For an explanation of numbers, see Figure 4.

accord with the observed half-life of temozolomide in phosphate buffer (pH 7.4 at 37 °C) being comparable with its mean plasma half-life in patients.[5] The enhanced clinical activity of temozolomide over the other prodrug of MTIC (DTIC) must therefore be due to more effective generation of unstable MTIC inside cell nuclei.

Experimental Section

Molecular Modeling. The published crystal structures of temozolomide[4] and mitozolomide[12] were the starting templates for the construction of structures of carbamoyl-substituted benzo-1,2,3-triazinones and related heterocycles (Figure 2) using the modeling package Chem-X.[28] The structures were then optimized using the *ab initio* molecular orbital package GAMESS[29] with the 321-G basis set. The similarities of the analogues were measured with the similarity program ASP.[30] For the electrostatic similarities, the structures were optimized with the Hodgkin potential similarity algorithm.[13]

Synthesis. All new compounds were characterized by elemental microanalysis (C, H, and N values) and mass spectrometry (recorded on a V.G. Micromass 12B instrument at 70 eV; source temperature 250–300 °C). FAB and high-resolution FAB mass spectra were run at the EPSRC Mass Spectrometry Service Centre, University of Wales, Swansea. UV spectra were recorded on a Cecil CE 5095 spectrometer in 95% ethanol solutions. IR spectra were determined on either a Mattson 2020 Galaxy Series FT spectrometer or a Perkin Elmer 1310 infrared spectrometer as either Nujol mulls or KBr discs. NMR spectra were recorded in DMSO-d_6 (unless otherwise indicated) on Jeol GX 500, Bruker ARX 400, or Bruker ARX 250 spectrometers. J values are recorded in hertz (Hz). TLC systems for routine monitoring of reaction mixtures and confirming the homogeneity of analytical samples employed Kieselgel $60F_{254}$ (0.25 mm) with either $CHCl_3$ or $CHCl_3$–2% ethanol as developing solvents. Sorbsil silica gel C 60-H (40–60 μm) was used for flash chromatography.

Synthesis of Imidazo-1,2,3,5-tetrazinones. 1,6-Dinitro-5*H*,10*H*-diimidazo[1,5-*a*:1′-*d*]pyrazine-5,10-dione (17). A mixture of 5-nitroimidazole-4-carboxylic acid (**15**)[31] (0.6 g), anhydrous toluene (8 mL), and thionyl chloride (1.3 mL) was refluxed (3 h) and evaporated to yield an oily residue which was triturated in toluene:petroleum ether (60–80 °C, 1:1, 10 mL). The brown solid (0.43 g) had mp 247–249 °C (lit.[32] mp 249–251 °C) and IR 1750 (C=O), 1540 (NO_2) cm^{-1} but was shown by mass spectrometry to be a mixture of **17** (M^+ 278), **18** (M^+ 267/269, 3:1), and **19** (M^+ 256/258/260, 9:6:1).

3-(2-Chloroethyl)-*N*-phenyl-4-oxoimidazo[5,1-*d*]-1,2,3,5-tetrazine-8-carboxamide (22). This compound was prepared in 95% yield from the 8-carbonyl chloride **21** and aniline by the method of Horspool.[16]

Similarly prepared from **21** and the appropriate aminobenzamides were the following.

3-(2-Chloroethyl)-*N*-(2-carbamoylphenyl)-4-oxoimidazo-[5,1-*d*]-1,2,3,5-tetrazine-8-carboxamide (23): from 2-aminobenzamide (15%); mp 179–181 °C dec; IR 3525–3100 br (NH), 1742, 1685, 1642 (C=O) cm^{-1}. Anal. ($C_{14}H_{12}ClN_7O_3$) C, H, N.

3-(2-Chloroethyl)-*N*-(3-carbamoylphenyl)-4-oxoimidazo-[5,1-*d*]-1,2,3,5-tetrazine-8-carboxamide (24): from 3-aminobenzamide (21%); mp 250–252 °C dec; IR 3435, 3368, 3187 br (NH), 1740, 1661 (C=O) cm^{-1}. Anal. ($C_{14}H_{12}ClN_7O_3$) C, H, N.

3-(2-Chloroethyl)-*N*-(4-carbamoylphenyl)-4-oxoimidazo-[5,1-*d*]-1,2,3,5-tetrazine-8-carboxamide (25): from 4-aminobenzamide (24%); mp 249–250 °C dec; IR 3378 br, 3168 br (NH), 1734, 1677, 1655 (C=O) cm^{-1}. Anal. ($C_{14}H_{12}ClN_7O_3$) C, H, N.

3-(2-Chloroethyl)-*N*-(2,4-dicarbamoylphenyl)-4-oxoimidazo[5,1-*d*]-1,2,3,5-tetrazine-8-carboxamide (26): from 2-amino-5-carbamoylbenzamide (32%); crystallized from 1-methylpyrrolidin-2-one; mp 292–295 °C dec; IR 3378 br, 3192 br (NH), 1741, 1675, 1654 (C=O) cm^{-1}. Anal. ($C_{15}H_{13}ClN_8O_4 \cdot 0.5C_5H_9NO$) C, H, N.

3-(2-Chloroethyl)-*N*-[4-(2-amino-3,4-dihydro-4-oxopyrimidin-5-yl)phenyl]-4-oxoimidazo[5,1-*d*]-1,2,3,5-tetrazine-8-carboxamide (27): from 2-amino-5-phenylpyrimidin-4(3*H*)-one (28%); crystallized from a mixture of 1-methylpyrrolidin-2-one and ether; mp >320 °C dec; IR 3500–3000 br (NH), 1746, 1690, 1654 (C=O) cm^{-1}. Anal. ($C_{17}H_{14}ClN_9O_3 \cdot C_5H_9NO$) C, H, N.

Spermidine–Temozolomide (28) and Mitozolomide (29) Conjugates. Temozolomide-8-carbonyl chloride[16] was dissolved in dry dichloromethane (10 mL) under nitrogen and cooled to −40 °C. A solution of N^1,N^8-bis(*tert*-butoxycarbonyl)-N^4-(3-aminopropyl)spermidine[32] (0.94 g) and triethylamine (0.26 g) in dichloromethane (10 mL) was added to the acid chloride solution at −40 °C over 5 min with rapid stirring. The solution was stirred at −40 °C for 2 h and then allowed to warm to room temperature overnight. The solution was recooled to −40 °C, TFA (1.5 g) added, and the solution allowed to warm to room temperature. Solvent and excess TFA were removed by evaporation *in vacuo*, and the orange residue was dissolved in 1 M HCl (100 mL). The acid solution was shaken with chloroform (10 mL) to remove a small oily fraction, and the aqueous layer was loaded onto a Dowex 50 X2-200 ion exchange column. The column was washed with 1 M HCl (400 mL), 1.25 M HCl (100 mL), 1.5 M HCl (450 mL), and 1.8 M HCl (450 mL). Evaporation of the 1.5 and 1.8 M HCl eluents yielded a pink foam of the spermidine–temozolomide conjugate **28** as a hygroscopic trihydrochloride salt (30%). ^{1}H NMR (500 MHz, homonuclear correlations by COSY45) δ 11.02 (br s, 1H, N(4″)H), 8.77 (s, 1H, 6-H), 8.52 (br t, 1H, J = 5.8, CON*H*), 8.31 (br s, 3H, N(1″)H), 8.20 (br s, 3H, N(8″)H), 3.87 (s, 3H, CH_3), 3.42 (q, 2H, J = 6.5, 3′-H), 3.23 (m, 2H, 3″-H), 3.09–3.07 (m, 4H, 1′-H, 5″-H), 2.92 (sextet, 2H, J = 6.2, 1″-H), 2.82 (sextet 2H, J = 6.6, 8″-H), 2.10 (quint, 2H, J = 7.7, 2″-H),

2.05 (quint, 2H, J = 7.7, 2′-H), 1.85 (br quint, 2H, J = 8.0, 6″-H), 1.66 (quint, 2H, J = 7.5, 7″-H); ^{13}C NMR (62.9 MHz, assignments by DEPT135, HETCOR) δ 160.7 (CONH), 139.8 (C-4), 135.1 (C-8a), 130.8 (C-8), 129.2 (C-6), 51.7 (C-5″), 50.6 (C-1′), 49.6 (C-3″), 39.3 (C-8″), 36.8 (C-1″), 36.7 (C-3′), 36.4 (CH_3), 24.7 (C-7″), 23.9 (C-2′), 21.8 (C-2″), 20.4 (C-6″); FAB MS m/z 380.252 (M + H$^+$), $C_{16}H_{30}N_9O_2$ requires 380.252.

Similarly prepared, from mitozolomide-8-carbonyl chloride (**21**), was the spermidine–mitozolomide conjugate **29** as a hydroscopic trihydrochloride salt (74%); ^{1}H NMR (400 MHz) δ 9.45 (1H, br s, N(4″)H), 8.82 (1H, s, 6-H), 8.53 (1H, t, J = 5.8, CONH), 8.30 (3H, br, N(1″)H), 8.19 (3H, br, N(8″)H), 4.64 (2H, t, J = 6.1, CH_2CH_2Cl), 4.04 (2H, t, J = 6.1, CH_2CH_2Cl), 3.43 (2H, quint, J = 6.3, 3′-H), 3.25 (2H, m, 3″-H), 3.10 (4H, m, 5″-H, 1′-H), 2.93 (2H, m, 1″-H), 2.83 (2H, m, 8″-H), 2.14 (2H, m, 2″-H), 2.08 (2H, m, 2′-H), 1.85 (2H, quint, J = 7.7, 6″-H), 1.68 (2H, quint, J = 7.3, 7″-H); ^{13}C NMR (62.9 MHz) δ 160.0 (CONH), 139.2 (C-4), 134.1 (C-8a), 131.4 (C-8), 129.4 (C-6), 51.6 (C-1′), 50.5 (C-5″), 50.2 (CH_2CH_2Cl), 49.5 (C-3), 41.6 (CH_2CH_2Cl), 38.3 (C-8″), 36.6 (C-3′), 36.5 (C-1″), 24.4 (C-7″), 23.6 (C-2′), 21.6 (C-2″), 20.3 (C-6″); FAB MS m/z 428.230 (M + H$^+$), $C_{17}H_{31}{}^{35}ClN_9O_2$ requires 428.229.

Synthesis of Benzo-1,2,3-triazinones by Nitrosation of *o*-Aminobenzamides. 2-Nitrobenzene-1,3-dicarboxamide (32). A mixture of the 1,3-dicarboxylic acid **30** (1.68 g), thionyl chloride (10 mL), and DMF (0.1 mL) was refluxed for 12 h. The solution was evaporated and the residue triturated with toluene (10 mL) and re-evaporated. The resulting solid was stirred at 25 °C with concentrated aqueous ammonia for 24 h. The dicarboxamide **32** (0.54 g, 32%) crystallized from water as colorless needles: mp 288–290 °C (lit.[33] mp 278–280 °C).

2-Nitrobenzene-1,4-dicarboxamide (33): similarly prepared from the 1,4-dicarboxylic acid **31** (61%) which crystallized from water as yellow needles; mp 262–264 °C; m/z 209 (M$^+$). Anal. ($C_8H_7N_3O_4$) C, H, N.

2-Aminobenzene-1,3-dicarboxamide (34). Hydrogenation of **32** in DMF over a palladium-charcoal catalyst gave the amine **34** (66%) as colorless crystals from water, mp 290–292 °C. Anal. ($C_8H_9N_3O_2$) C, H, N.

2-Aminobenzene-1,4-dicarboxamide (35): similarly prepared (62%) by catalytic hydrogenation of **33**: mp 275–277 °C, from water; MS (EI) m/z 179 (M$^+$). Anal. ($C_8H_9N_3O_2$) C, H, N.

3,4-Dihydro-4-oxobenzo-1,2,3-triazine-7-carboxamide (36). The amino dicarboxamide **35** (0.25 g) in DMF (3 mL) was added to a solution of sodium nitrite (0.12 g) in 0.5 M HCl (12 mL) at 0 °C. The mixture was stirred (1 h), basified with aqueous ammonia, and reacidified to pH 2. The triazinone **36** (0.2 g) crystallized from aqueous ethanol as white needles: mp 273–275 °C dec; IR 3369 br (NH), 1692, 1673 (C=O) cm^{-1}; MS (EI) m/z 190 (M$^+$). Anal. ($C_8H_6N_4O_2$) C, H, N.

3,4-Dihydro-4-oxobenzo-1,2,3-triazine-8-carboxamide (37): similarly prepared from **34** in 75% yield; mp 254–256 °C dec; IR 3388, 3108 br (NH), 1685, 1657 (C=O) cm^{-1}; MS (EI) m/z 190 (M$^+$). Anal. ($C_8H_6N_4O_2$) C, H, N.

7-Carboxyisatoic Anhydride (40). 2-Aminobenzene-1,4-dicarboxylic acid (**39**) (1.5 g) and triphosgene (0.82 g, 2.8 mmol) in dry THF (40 mL) were heated at 40-50 °C for 3 h under nitrogen. The solution was filtered, and the isatoic anhydride **40** (1.67 g, 97%) precipitated by the addition of hexane: mp 320–322 °C; MS (EI) m/z 207 (M$^+$). Anal. ($C_9H_5NO_5$) C, H, N.

8-Carboxyisatoic anhydride (41): similarly prepared from **38** in 98% yield; mp 245–250 °C sublimination; MS (EI) m/z 207 (M$^+$). Anal. ($C_9H_5NO_5$) C, H, N.

2-Amino-3-(*N*-methylcarbamoyl)benzoic Acid (42). 8-Carboxyisatoic anhydride (**41**) (0.9 g) was added portionwise to a stirred solution of 40% aqueous methylamine (1.5 mL) in water (25 mL) at 25 °C over 0.5 h. The benzoic acid **42** was collected (0.69 g, 79%) and crystallized from aqueous ethanol as colorless needles: mp 222–224 °C; MS (EI) m/z 194 (M$^+$). Anal. ($C_9H_{10}N_2O_3$) C, H, N.

Similarly prepared from **41** were the following.

2-Amino-3-[*N*-(2-chloroethyl)carbamoyl]benzoic acid (43): with 2-chloroethylamine (prepared by the addition of triethylamine in ethanol to a solution of 2-chloroethylamine hydrochloride in water); 58% yield as white needles; mp 200–202 °C (from aqueous acetone); MS (EI) m/z 242/244 (M$^+$). Anal. ($C_{10}H_{11}ClN_2O_3$) C, H, N.

2-Amino-3-(*N*-ethylcarbamoyl)benzoic acid (44): with 75% aqueous ethylamine; 85% yield; mp 233–235 °C (from water); MS (EI) m/z 208 (M$^+$). Anal. ($C_{10}H_{12}N_2O_3$) C, H, N.

***N*-(2-Amino-3-carboxybenzoyl)glycine methyl ester (45):** 67% yield; with glycine methyl ester (synthesized by the addition of triethylamine in ethanol to a solution of glycine methyl ester hydrochloride in water); mp 192–193 °C (from water); MS (EI) m/z 252 (M$^+$). Anal. ($C_{10}H_{12}N_2O_3$) C, H, N.

2-Amino-3-(*N*-phenylcarbamoyl)benzoic acid (46): 62%; with aniline in dioxane; mp 248 °C (from aqueous ethanol); MS (EI) m/z 256 (M$^+$). Anal. ($C_{14}H_{12}N_2O_3$) C, H, N.

Similarly prepared from **40** were the following.

3-Amino-4-(*N*-methylcarbamoyl)benzoic acid (47): 62% yield; with aqueous methylamine; mp 217–218 °C as yellow plates (from aqueous ethanol); MS (EI) m/z 194 (M$^+$). Anal. ($C_9H_{10}N_2O_3$) C, H, N.

3-Amino-4-(*N*-ethylcarbamoyl)benzoic acid (48): 51%; with 75% aqueous ethylamine; mp 200–201 °C (from water); MS (EI) m/z 208 (M$^+$). Anal. ($C_{10}H_{12}N_2O_3$) C, H, N.

3-Amino-4-(*N*-phenylcarbamoyl)benzoic acid (49): 65%; with aniline in dioxane; mp 231–233 °C (from aqueous ethanol); MS (EI) m/z 256 (M$^+$). Anal. ($C_{14}H_{12}N_2O_3$) C, H, N.

3,4-Dihydro-4-oxo-3-methylbenzo-1,2,3-triazine-7-carboxylic Acid (50). The *N*-methylamide **47** (0.6 g) and anhydrous sodium carbonate (0.18 g) were warmed in water (15 mL) until all the methylamide had dissolved. The solution was cooled to room temperature and sodium nitrite (0.27 g) added. The solution was poured into 0.5 M hydrochloric acid at 0 °C, and the mixture was stirred at 0 °C for 1 h. Acidification of the mixture to pH 2 liberated the benzotriazinone **50**, which crystallized from aqueous ethanol as colorless needles (81%): mp 245–247 °C dec; IR 3220–2600 br (OH), 1692 (C=O) cm^{-1}; m/z 205 (M$^+$). Anal. ($C_9H_7N_3O_3$) C, H, N.

Similarly prepared were the following.

3,4-Dihydro-4-oxo-3-ethylbenzo-1,2,3-triazine-7-carboxylic acid (51): from the *N*-ethylamide **48** in 75% yield as colorless plates from aqueous ethanol; mp 232–235 °C dec; IR 3220–2600 br (OH), 1692 (C=O) cm^{-1}. Anal. ($C_{10}H_9N_3O_3$) C, H, N.

3,4-Dihydro-4-oxo-3-phenylbenzo-1,2,3-triazine-7-carboxylic acid (52): from the *N*-phenylamide **49** in 69% yield as colorless plates from aqueous ethanol; mp 237–239 °C dec; IR 3250–2400 br (OH), 1694 (C=O) cm^{-1}. Anal. ($C_{14}H_9N_3O_3$) C, H, N.

3,4-Dihydro-4-oxo-3-methylbenzo-1,2,3-triazine-8-carboxylic acid (53): from **42** in 77% yield; mp 188–189 °C dec; IR 3250–2500 br (OH), 1703 (C=O) cm^{-1}. Anal. ($C_9H_7N_3O_3$) C, H, N.

3,4-Dihydro-4-oxo-3-(2-chloroethyl)benzo-1,2,3-triazine-8-carboxylic acid (54): from **43** in 71% yield; mp 163–165 °C dec; IR 3250–2500 br (OH), 1703 (C=O) cm^{-1}; MS (EI) m/z 253/255 (M$^+$). Anal. ($C_{10}H_8ClN_3O_3$) C, H, N.

3,4-Dihydro-4-oxo-3-ethylbenzo-1,2,3-triazine-8-carboxylic acid (55): from the *N*-ethylamide **44** in 74% yield as colorless plates from aqueous ethanol; mp 145–146 °C dec; IR 3250–2400 (OH), 1685 (C=O) cm^{-1}; MS (EI) m/z 219 (M$^+$) ($C_{10}H_9N_3O_3$) C, H, N.

***N*-(8-Carboxy-3,4-dihydro-4-oxobenzo-1,2,3-triazin-3-yl)glycine methyl ester (56):** from **45** in 59% yield as colorless plates from water; mp 113–115 °C dec; IR 3100–2600 br (OH), 1741 (O–C=O), 1701 (C=O) cm^{-1}; MS (EI) m/z 263 (M$^+$). Anal. ($C_{11}H_9N_3O_5$) C, H, N.

3,4-Dihydro-4-oxo-3-phenylbenzo-1,2,3-triazine-8-carboxylic acid (57): from the *N*-phenylamide **46** in 82% yield as colorless plates from aqueous ethanol; mp 185 °C dec; IR 3200–2450 br (OH), 1701 (C=O), 1689 (C=O) cm^{-1}; MS (EI) m/z 267 (M$^+$). Anal. ($C_{14}H_9N_3O_3$) C, H, N.

3,4-Dihydro-4-oxo-3-methylbenzo-1,2,3-triazine-7-carboxamide (7). A mixture of the carboxylic acid **50** (0.45 g),

thionyl chloride (5 mL), and DMF (0.1 mL) was refluxed (3 h). Removal of excess thionyl chloride gave a residue which was dissolved in dry THF (10 mL) and stirred with concentrated aqueous ammonia (5 mL) at 25 °C for 12 h. The solid carboxamide **7** (71%) was collected, washed with water, and crystallized from aqueous ethanol as colorless needles: mp 277–280 °C dec; IR 3420 br, 3300 br (NH), 1680, 1655 (C=O) cm^{-1}; MS (EI) m/z 207 (M^+). Anal. ($C_9H_8N_4O_2$) C, H, N.

Similarly prepared were the following.

3,4-Dihydro-4-oxo-3-ethylbenzo-1,2,3-triazine-7-carboxamide (58): from the carboxylic acid **51** in 66% yield as colorless plates from aqueous ethanol; mp 260–262 °C dec; IR 3375 br (NH), 1698, 1658 (C=O) cm^{-1}; MS (EI) m/z (M^+) 218. Anal. ($C_{10}H_{10}N_4O_2$) C, H, N.

3,4-Dihydro-4-oxo-3-phenylbenzo-1,2,3-triazine-7-carboxamide (59): from **52** in 54% yield as colorless crystals from aqueous ethanol; mp 266–267 °C dec; IR 3400 br (NH), 1702, 1665 (C=O) cm^{-1}; MS (EI) m/z 266 (M^+). Anal. ($C_{14}H_{10}N_4O_2$) C, H, N.

3,4-Dihydro-4-oxo-3-methylbenzo-1,2,3-triazine-8-carboxamide (9): from the acid **53** in 69% yield; mp 200–202 °C dec; IR 3363 br, 3207 br (NH), 1699, 1679 (C=O) cm^{-1}; MS (EI) m/z 204 (M^+). Anal. ($C_9H_8N_4O_2$) C, H, N.

3,4-Dihydro-4-oxo-3-(2-chloroethyl)benzo-1,2,3-triazine-8-carboxamide (10): from **54** in 71% yield as cream needles; mp 211–212 °C dec; IR 3338 br, 3164 (NH), 1696, 1684, 1673 (C=O) cm^{-1}; MS (EI) m/z 252/253 (M^+). Anal. ($C_{10}H_9ClN_4O_2$) C, H, N.

3,4-Dihydro-4-oxo-3-ethylbenzo-1,2,3-triazine-8-carboxamide (60): from **55** in 72% yield as colorless plates from aqueous ethanol; mp 196 °C dec; IR 426, 3157 br (NH), 1689, 1654 (C=O) cm^{-1}; MS (EI) m/z 218 (M^+). Anal. ($C_{10}H_{10}N_4O_2$) C, H, N.

***N*-(8-Carbamoyl-3,4-dihydro-4-oxobenzo-1,2,3-triazin-3-yl)glycine amide (61):** from **56** in 56% yield as a white solid from aqueous ethanol; mp 286 °C dec; IR 3374, 3344 br, 3208 br (NH), 1701, 1693, 1685, 1674 (C=O) cm^{-1}; MS (EI) m/z 247 (M^+). Anal. ($C_{10}H_9N_5O_3$) C, H, N.

3,4-Dihydro-4-oxo-3-phenylbenzo-1,2,3-triazine-8-carboxamide (62): from **57** in 82% yield as cream needles from aqueous ethanol; mp 234–236 °C dec; IR 3407 br, 3201 br (NH), 1702, 1665 (C=O) cm^{-1}; MS (EI) m/z 266 (M^+). Anal. ($C_{14}H_{10}N_4O_2$) C, H, N.

Synthesis of Benzo-1,2,3-triazinones by Cyclization of Methyl Triazenyl-Substituted Carboxylates. Dimethyl 2-(3-Methyltriazen-1-yl)benzene-1,4-dicarboxylate (64). A suspension of the diester **63** (0.5 g) in 0.5 M HCl (15 mL) at 0 °C was diazotized by the addition of sodium nitrite (0.19 g) in water (1 mL). The diazonium solution was treated with 40% aqueous methylamine solution (0.7 mL), and the precipitate was immediately collected, washed with ice–water, and extracted into chloroform. Evaporation of the dried (sodium sulfate) solvent gave the triazene **64** as a pale yellow solid (70%): mp 116–118 °C dec; IR 3265 (NH), 1725, 1695 (C=O) cm^{-1}. Anal. ($C_{11}H_{13}N_3O_4$) C, H, N.

Attempted crystallization of the triazene **64** from 95% aqueous ethanol gave methyl 3,4-dihydro-4-oxo-3-methylbenzo-1,2,3-triazine-7-carboxylate (**66**) in 74% yield: mp 144–145 °C dec; IR 1710, 1680 (C=O); MS (EI) m/z 219 (M^+). Anal. ($C_{10}H_9N_3O_3$) C, H, N.

Treatment of the triazine carboxylate **66** with methanolic ammonia for 48 h at 25 °C gave the carboxamide **7** (59%), identical (IR) to a sample previously prepared from the carboxylic acid **50** (see above).

Dimethyl 2-(3-Phenyltriazen-1-yl)benzene-1,4-dicarboxylate (65). This was prepared by coupling diazotized dimethyl 2-aminobenzene-1,4-dicarboxylate (**63**) with aniline in sodium acetate-buffered solution at 0 °C. The triazene **65** crystallized from aqueous ethanol as yellow needles (80%): mp 155–156 °C dec; IR 3225 (NH), 1690 (C=O) cm^{-1}. Anal. ($C_{16}H_{15}N_3O_4$) C, H, N.

Methyl 3,4-Dihydro-4-oxo-3-phenylbenzo-1,2,3-triazine-7-carboxylate (67). The triazene **65** (0.5 g) was boiled in 70% aqueous ethanol (10 mL) for 2 h. The cooled mixture deposited yellow crystals of the triazine carboxylate **67** (76%): mp 148–149 °C dec; IR 1715, 1695 (C=O) cm^{-1}; MS (EI) m/z 281 (M^+). Anal. ($C_{15}H_{11}N_3O_3$) C, H, N. The same triazine carboxylate (82%) was formed when the triazene **65** was refluxed in methanol containing 2% piperidine.

Ethyl 3,4-Dihydro-4-oxo-3-phenylbenzo-1,2,3-triazine-7-carboxylate (68). This triazine carboxylate was formed (66%) when **65** (0.5 g) was boiled in 95% ethanol containing 2% piperidine for 1 h. The cooled mixture deposited yellow crystals: mp 156–158 °C dec; IR 1720, 1680 (C=O) cm^{-1}; MS (EI) m/z 295 (M^+). Anal. ($C_{16}H_{13}N_3O_3$) C, H, N.

When triazene **65** was boiled in a mixture of ethanol:water: piperidine (70:28:2) the product was 3,4-dihydro-4-oxo-3-phenylbenzo-1,2,3-triazine-7-carboxylic acid (**52**) (45%), identical to the aforementioned sample.

Synthesis of a Pyrazolo[4,3-*d*]-1,2,3-triazinone and a Pyrazolo[5,1-*d*]-1,2,3,5-tetrazinone. Dimethyl 4-Diazopyrazole-3,5-dicarboxylate (70). A solution of dimethyl 4-aminopyrazole-3,5-dicarboxylate (**69**)[35] (0.2 g) in 0.25 M HCl (15 mL) was diazotized at 0 °C with sodium nitrite (0.086 g). The stirred (1 h) reaction mixture was neutralized with 1 M sodium acetate solution and extracted with chloroform (3 × 10 mL). The organic extracts were dried (anhydrous sodium sulfate) and evaporated to give a yellow oil which solidified when triturated with hexane. Unstable diazopyrazole **70** (45%): mp 129–130 °C dec; IR 2196 (C=N=N), 1749, 1713 (C=O) cm^{-1}; ^1H NMR ($CDCl_3$) δ 4.05 (6H, s, 2 × CO_2Me).

***N*-Methyl 3,4-Dihydro-4-oxo-3-methyl-5*H*-pyrazolo[4,3-*d*]-1,2,3-triazine-7-carboxamide (72).** The diazopyrazole **70** (0.1 g) was stirred with a saturated solution of methylamine in ethyl acetate (10 mL) at 25 °C for 24 h, and the solid was collected. Purification of the crude product by flash chromatography using ethyl acetate as eluent gave the pyrazolotriazine **72** as a white solid (0.010 g, 5%): mp 179–181 °C; IR 3430 br, 3127 br (NH), 1703, 1672 (C=O) cm^{-1}; MS (EI) m/z 208 (M^+). Anal. ($C_7H_8N_6O_2$) C, H, N.

3-Benzyl-3,4-dihydro-4-oxopyrazolo[5,1-*d*]-1,2,3,5-tetrazine-8-carboxamide (74). 5-Diazopyrazole-4-carboxamide (**73**)[24] (0.3 g) was stirred with benzyl isocyanate (0.28 mL) in dry DMSO (5 mL) in a light-protected flask for 7 h. Addition of water (5 mL) precipitated the pyrazolotetrazinone (0.29 g) which was collected and washed with ethyl acetate: mp 220–221 °C dec; IR 3441, 3204, (NH), 3106 (CH), 1746, 1690 (C=O) cm^{-1}; MS (EI) m/z 270 (M^+). Anal. ($C_{12}H_{10}N_6O_2$) C, H, N.

Hydrolysis of Mitozolomide in the Presence of Nucleic Acids and Nucleotides. Synthetic nucleic acid oligomers were purchased from Sigma Chemical Co., Ltd., Poole, U.K., and HPLC grade solvents were obtained from Fisons, Loughborough, U.K. HPLC analyses were performed using a Waters 600E gradient solvent delivery system fitted with a Merck 250 Lichrosorb RP select B column and a Lichrocart reversed-phase C-18 endcapped guard column and monitored at 325 nm. Hydrolyses were performed in glass screw-capped vials in a total volume of 3 mL and monitored for approximately three half-lives. Aliquots (10 μL) were removed from the incubation mixture, injected directly onto the column using a Waters WISP 710B automatic injection sampler, and eluted with a mobile phase of acetic acid (0.5%) in water/methanol (70:30) at a flow rate of 1 mL/min for 10 min. Typically, mitozolomide had a retention time of 4.8 min.

***In Vitro* Growth Inhibition. (a) Mouse TLX5 Lymphoma Cells.** TLX5 lymphoma cells were maintained in exponential growth phase at 2 × 10^4 cells/mL in RPMI 1640 supplemented with 15% fetal calf serum. Aliquots (2 mL) of the cells were plated out into six wells of multiwell dishes and treated with 10 μL of the required drug solutions in DMSO, with three replicates for each drug concentration. The control incubates were composed of cells treated with 10 μL of DMSO. After being incubated for 72 h at 37 °C in an atmosphere of 5% CO_2, the cells were counted using a Coulter Laboratories ZM counter. Results were plotted as percent of control population growth (data not shown), from which the IC_{50} values (μM) were calculated.

(b) Human Raji and GM892A Cells. Raji and GM892A cells were routinely cultured in RPMI 1640 medium supplemented with 10% fetal calf serum and 1% L-glutamine. Cells were seeded at 0.8 × 10^5 cells/mL in Nunc 24-well plates and treated with a range of drug concentrations. Drugs were

dissolved in DMSO and added so that the DMSO concentration did not exceed 0.5%. A minimum of three cell populations were treated for each drug concentration, and cell numbers were duplicate-counted following a 72 h incubation period. The growth of the treated cell population was compared to the growth of a solvent-treated control cell population, after subtraction of the seed number from the final cell counts. IC_{50} values (μM) were calculated as above.

Effect of Pre-exposure to GM892 Cells by Benzo-1,2,3-triazinones on the Cytotoxicity of Temozolomide. GM892A cells were seeded at 0.8×10^5 cells/mL and treated with a range of concentrations of potential antagonists as described above. After incubation for 2 h at 37 °C, the cells were centrifuged, washed with PBS, resuspended in media, and then aliquoted into Nunc 24-well plates before being challenged with temozolomide. Cells were incubated for 3–4 days at 37 °C. The ability of temozolomide to inhibit growth of cells pretreated with the inactive benzo-1,2,3-triazinones was compared with the inhibition elicited by temozolomide alone in solvent-treated controls.

Determination of Guanine N-7 Alkylation Sites in Defined DNA Sequences. (a) DNA Fragment Isolation and Labeling. The basic procedure was as described by Hartley et al.[26] *Bam*HI-digested pBR322 DNA was 5′-^{32}P-end-labeled by standard methods and a 276-bp *Bam*HI-*Sal*I fragment was isolated following further cleavage with *Sal*I. A 346-bp *Hind*III-*Bam*HI fragment of pBR322 DNA 5′-labeled at the *Hind*III restriction site was prepared by the same method following initial cutting by *Hind*III.

(b) Fragment Alkylation and Piperidine Cleavage. The DNA fragment (5000 cpm/sample) was alkylated in 25 mM triethanolamine HCl–1 mM EDTA at pH 7.2 at 37 °C for 2 h using a range of concentrations of drug in a final reaction volume of 50 μL (drugs were dissolved in DMSO to give a concentration of 2% DMSO in the final reaction mixture). Following ethanol precipitation and washing, the alkylated DNA was treated with 100 μL of a fresh solution of 10% piperidine at 90 °C for 15 min to produce strand breaks specifically at the sites of guanine N-7 alkylation. The DNA fragments were then dissolved in formamide dye solution, heated at 90 °C for 2 min, and separated using electrophoresis on 0.4 mm × 90 cm × 20 cm 6% denaturing polyacrylamide gels containing 7 M urea and a tris–boric acid–EDTA (TBE) buffer system. Gels were prerun at 3000 V for 30 min; samples were run into the gel at 1000 V for 5 min and then for 3 h at approximately 3000 V, maintaining a temperature of 55–65 °C. Fragments were visualized by autoradiography of the dried gel and relative band intensities determined by microdensitometry.

Measurement of the Sequence Specificity using *Taq* DNA Polymerase Stop Assay. The sequence specificity of covalent DNA modification by temozolomide (1) and ethazolastone (3) was examined using a polymerase stop assay.[35] *Bam*HI-*Sal*I DNA isolated following restriction digestion of pBR322 DNA was reacted with drug in triethanolamine–1 mM EDTA, pH 7.2, at 37 °C for 1 h in a final volume of 50 μL. After ethanol precipitation and lyophilization, the fragment was used as a template for extension of a 5′-^{32}P-end-labeled 20-base oligonucleotide primer of sequence 5′-TATGCGACTC-CTGCATTAGG-3′. The polymerase chain reaction was carried out in a total volume of 100 μL containing 0.5 μg of alkylated or control DNA, 0.25 ng of labeled primer, 10 μL of 10× buffer (670 mM Tris, pH 8.4, 20 mM $MgCl_2$), 250 μM of each dNTP, and 1 U of *Taq* polymerase. The samples were mixed and overlaid with 2 drops of mineral oil and then incubated in a thermal cycler. A linear amplification procedure was carried out for 30 cycles, each consisting of 1 min denaturation at 95 °C, 2 min annealing at 60 °C, and 2 min chain elongation at 72 °C. Following completion of the cycles, samples were cooled on ice, extracted with chloroform/isoamyl alcohol (24:1), and precipitated with ethanol. DNA fragments were separated by denaturing polyacrylamide gel electrophoresis and visualized by autoradiography as described for the piperidine cleavage method.

Acknowledgment. This study was supported by the Cancer Research Campaign, U.K. We thank Ms. H. Hussey for conducting the TLX5 lymphoma *in vitro* cytotoxicity tests and Mr. K. Farnell for technical support of the synthetic work.

Supplementary Material Available: Base sequence of the *Bam*HI-*Sal*I fragment of pBR322 DNA (1 page). Ordering information is given on any current masthead page.

References

(1) Wheelhouse, R. T.; Wilman, D. E. V.; Thomson, W.; Stevens, M. F. G. Antitumour Imidazotetrazines. Part 31. The Synthesis of Isotopically Labelled Temozolomide and a Multinuclear (^{1}H, ^{13}C, ^{15}N) Magnetic Resonance Investigation of Temozolomide and Mitozolomide. *J. Chem. Soc., Perkin Trans. I* **1995**, 249–252.

(2) Stevens, M. F. G.; Hickman, J. A.; Langdon, S. P.; Chubb, D.; Vickers, L.; Stone, R.; Baig, G.; Goddard, C.; Gibson, N. W.; Slack, J. A.; Newton, C.; Lunt, E.; Fizames, C.; Lavelle, F. Antitumor Activity and Pharmacokinetics in Mice of 8-Carbamoyl-3-methylimidazo-[5,1-*d*]-1,2,3,5-tetrazin-4(3*H*)-one (CCRG 81045; M & B 39831), a Novel Drug with Potential as an Alternative to Dacarbazine. *Cancer Res.* **1987**, *47*, 5846–5852.

(3) Clark, A. S.; Stevens, M. F. G.; Sansom, C. E.; Schwalbe, C. H. Anti-tumor Imidazotetrazines. Part XXI. Mitozolomide and Temozolomide: Probes for the Major Groove of DNA. *Anti-Cancer Drug Des.* **1990**, *5*, 63–68.

(4) Lowe, P. R.; Sansom, C. E.; Schwalbe, C. H.; Stevens, M. F. G.; Clark, A. S. Antitumor Imidazotetrazines. 25. Crystal Structure of 8-Carbamoyl-3-methylimidazo[5,1-*d*]-1,2,3,5-tetrazin-4(3*H*)-one (Temozolomide) and Structural Comparisons with the Related Drugs Mitozolomide and DTIC. *J. Med. Chem.* **1992**, *30*, 3377–3382.

(5) Denny, B. J.; Wheelhouse, R. T.; Stevens, M. F. G.; Tsang, L. L. H.; Slack, J. A. An NMR and Molecular Modeling Investigation of the Mechanism of Activation of the Antitumor Drug Temozolomide and its Interaction with DNA. *Biochemistry* **1994**, *33*, 9045–9051.

(6) Stevens, M. F. G. Second-generation Azolotetrazinones. In *New Avenues in Developmental Cancer Chemotherapy*; Academic Press, Inc.: New York, 1987.

(7) Stevens, M. F. G.; Newlands, E. S. From Triazines and Triazenes to Temozolomide. *Eur. J. Cancer* **1993**, *29A*, 1045–1047.

(8) 'Reilly, S. M.; Newlands, E. S.; Glaser, M. G.; Brampton, M.; Rice-Edwards, J. M.; Illingworth, R. D.; Richards, P. G.; Kennard, C.; Colquhoun, I. R.; Lewis, P.; Stevens, M. F. G. Temozolomide: A New Oral Cytotoxic Chemotherapeutic Agent with Promising Activity Against Primary Brain Tumours. *Eur. J. Cancer* **1993**, *29A*, 940–942.

(9) Hartley, J. A.; Mattes, W. B.; Vaughan, K.; Gibson, N. W. DNA Sequence Specificity of Guanine-N7 Alkylations for a Series of Structurally Related Triazenes. *Carcinogenesis* **1988**, *9*, 669–674.

(10) Baer, J. C.; Freeman, A. A.; Newlands, E. S.; Watson, A. J.; Rafferty, J. A.; Margison, G. P. Depletion of O^6-Alkylguanine-DNA Alkyltransferase Correlates with Potentiation of Temozolomide and CCNU Toxiciy in Human Tumour Cells. *Br. J. Cancer* **1993**, *67*, 1299–1302.

(11) Tisdale, M. J. Antitumour Imidazotetrazines. XV. Role of Guanine O^6 Alkylation in the Mechanism of Cytotoxicity of Imidazotetrazinones. *Biochem. Pharmacol.* **1987**, *47*, 4884–4889.

(12) Lowe, P. R.; Schwalbe, C. H.; Stevens, M. F. G. Antitumour Imidazotetrazines. Part 5. Crystal and Molecular Structure of 8-Carbamoyl-3-(2-chloroethyl)imidazo[5,1-*d*]-1,2,3,5-tetrazin-4(3*H*)-one (Mitozolomide). *J. Chem. Soc., Perkin Trans. II* **1985**, 357–361.

(13) Hodgkin, E. E.; Richards, W. G. Molecular Similarity based on electrostatic potential and electric field. *Int. J. Quant. Chem.* **1987**, *14*, 105–110.

(14) Lunt, E.; Newton, C. G.; Smith, C.; Stevens, G. P.; Stevens, M. F. G.; Straw, C. G.; Walsh, R. J. A.; Warren, P. J.; Fizames, C.; Lavelle, F.; Langdon, S. P.; Vickers, L. M. Antitumor Imidazotetrazines. 14. Synthesis and Antitumor Activity of 6- and 8-Substituted Imidazo[5,1-*d*]-1,2,3,5-tetrazinones and 8-Substituted Pyrazolo[5,1-*d*]-1,2,3,5-tetrazinones. *J. Med. Chem.* **1987**, *30*, 357–366.

(15) Yasuda, N.; Okutsu, M.; Iwagami, H.; Nakamiya, T.; Takase, I. Imidazolecarboxylic Acid Derivatives. Eur. Pat Appl. 23045, 1981; *Chem. Abstr.* **1981**, *95*, 80954p.

(16) Horspool, K. R.; Stevens, M. F. G.; Newton, C. G.; Lunt, E.; Walsh, R. J. A.; Pedgrift, B. L.; Baig, G. U.; Lavelle, F.; Fizames, C. Antitumor Imidazotetrazines. 20. Preparation of the 8-Acid Derivative of Mitozolomide and Its Utility in the Preparation of Active Antitumor Agents. *J. Med. Chem.* **1990**, *33*, 1393–1399.

(17) Stevens, M. F. G. The Medicinal Chemistry of 1,2,3-Triazines. *Prog. Med. Chem.* **1976**, *13*, 205–269.

(18) Vaughan, K. The Effect of Electron-withdrawing Substituents on the Tautomerism Between 1-Aryl-3-methyltriazenes and 3-Aryl·1-methyltriazenes. *J. Chem. Soc., Perkin Trans. II* **1977**, 17–20.
(19) Vaughan, K.; Stevens, M. F. G. Monoalkyltriazenes. *Chem. Soc. Rev.* **1978**, *7*, 77–397.
(20) Slack, J. A.; Goddard, C. Antitumour Imidazotetrazines. VII. Quantitative Analysis of Mitozolomide in Biological Fluids by High Performance Liquid Chromatography. *J. Chromatogr.* **1985**, *337*, 178–181.
(21) Stevens, M. F. G.; Schwalbe, C. H.; Patel, N.; Gate, E. N.; Bryant, P. K. Structural Studies on Bio-active Compounds. Part 26. Hydrogen Bonding in the Crystal Structure of the *N*-methylformamide Solvate of the Immunomodulatory Agent 2-Amino-5-bromo-6-phenylpyrimidin-4-one (Bropirimine): Implications for the Design of Novel Anti-tumour Strategies. *Anti-Cancer Drug Des.* **1995**, in press.
(22) Harris, A. L.; Karran, P.; Lindahl, T. O^6-Methylguanine-DNA Methyltransferase of Human Lymphoid Cells: Structural and Kinetic Properties and Absence in Repair-Deficient Cells. *Cancer Res.* **1983**, *43*, 3247–3252.
(23) Gescher, A.; Threadgill, M. D. The Metabolism of Triazene Antitumor Drugs. *Pharmacol. Ther.* **1987**, *32*, 191–205.
(24) Cheng, C. C.; Elslager, E. F.; Werbel, L. M.; Priebe, S. R.; Leopold, W. R. Pyrazole Derivatives. 5. Synthesis and Antineoplastic Activity of 3-(2-chloroethyl)-3,4-dihydro-4-oxo-pyrazolo-[5,1-*d*]-1,2,3,5-tetrazine-8-carboxamide and Related Compounds. *J. Med. Chem.* **1986**, *29*, 1544–1547.
(25) Lamond, A. I.; Travers, A. A. Requirement for an Upstream Element for Optimal Transcription of a Bacterial tRNA gene. *Nature* **1983**, *305*, 248–250.
(26) Hartley, J. A.; Gibson, N. W.; Kohn, K. W.; Mattes, W. B. DNA Sequence Selectivity of Guanine-N7 Alkylation by Three Antitumor Chloroethylating Agents. *Cancer Res.* **1986**, *46*, 1943–1949.
(27) Holley, J. L.; Mather, A.; Wheelhouse, R. T.; Cullis, P. M.; Hartley, J. A.; Bingham, J. P.; Cohen, G. M. Targeting of Tumour Cells and DNA by a Chlorambucil-Spermidine Conjugate. *Cancer Res.* **1992**, *52*, 4190–4195.
(28) *Chem-X*; Chemical Design Ltd.: Chipping Norton, U.K., 1988.
(29) Schmidt, M. W.; Baldridge, K. K.; Boatz, J. A.; Elbert, S. T.; Gordan, M. S.; Jensen, J. H.; Koseki, S.; Matsunaga, N.; Nguyen, K. A.; Su, S. J.; Windus, T. L.; Dupuis, M.; Montgomery, J. A. General Atomic and Molecular Electronic Structure System. *J. Comput. Chem.* **1993**, *14*, 1347–1363.
(30) *ASP*; Oxford Molecular Ltd.: Oxford, U.K.
(31) Windaus, A.; Langebeck, W. 4(5)-Nitroimidazole-5(4)-carboxylic Acid. *Chem. Ber.* **1923**, *56B*, 683–686.
(32) Cohen, G. M.; Cullis, P. M.; Hartley, J. A.; Mather, A.; Symons, M. C. R.; Wheelhouse, R. T. Targeting of Cytotoxic Agents by Polyamines: Synthesis of a Chlorambucil-Spermidine Conjugate. *J. Chem. Soc., Chem. Commun.* **1992**, 298–300.
(33) Andrews, B. D.; Rae, I. D. Aromatic Amides. VI. Proton Resonance Spectra of Some 2-Substituted 1,3-Diphenylenediamines and their Diacyl Derivatives. *Aust. J. Chem.* **1971**, *24*, 413–422.
(34) Fagan, P. J.; Neidert, E. E.; Nye, M. J.; O'Hare, M. J.; Tang, W. Cycloadditions and Other Chemistry of 4-Oxygenated Pyrazoles. *Can. J. Chem.* **1979**, *57*, 904–912.
(35) Ponti, M.; Forrow, S. M.; Souhami, R. L.; D'Incalci, M.; Hartley, J. A. Measurement of the Sequence Specificity of Covalent DNA Modification by Antineoplastic Agents Using *Taq* DNA Polymerase. *Nucleic Acids Res.* **1991**, *19*, 2929–2933.
(36) Wheelhouse, R. T.; Denny, B. J.; Stevens, M. F. G. NMR and Molecular Modelling studies on the Mechanism of Action of the Antitumour Drug Temozolomide. *Contrib. Oncol.* **1995**, *49*, in press.

JM940789M